Supplemental Figures

A)

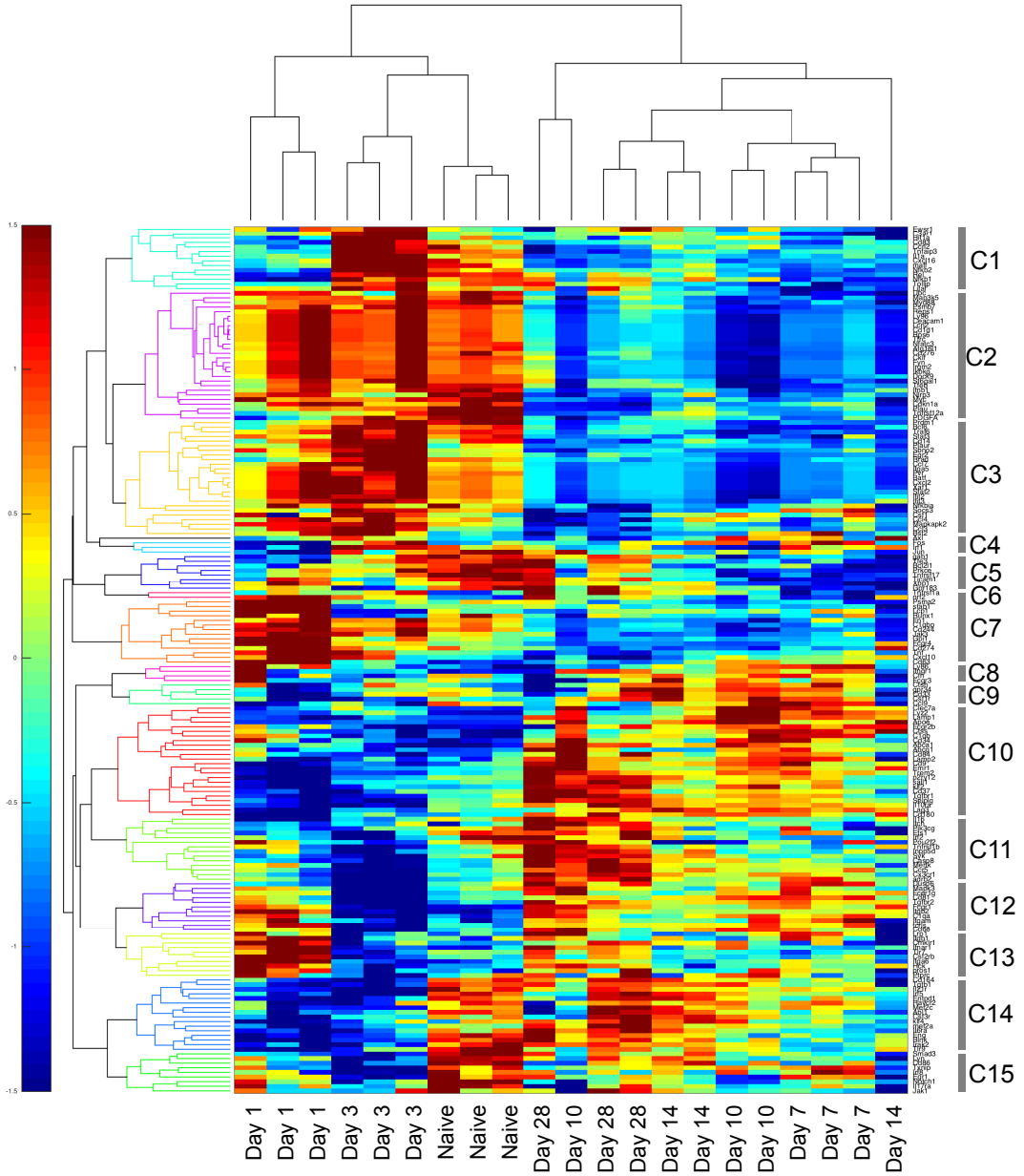

B) Clusters 1-4

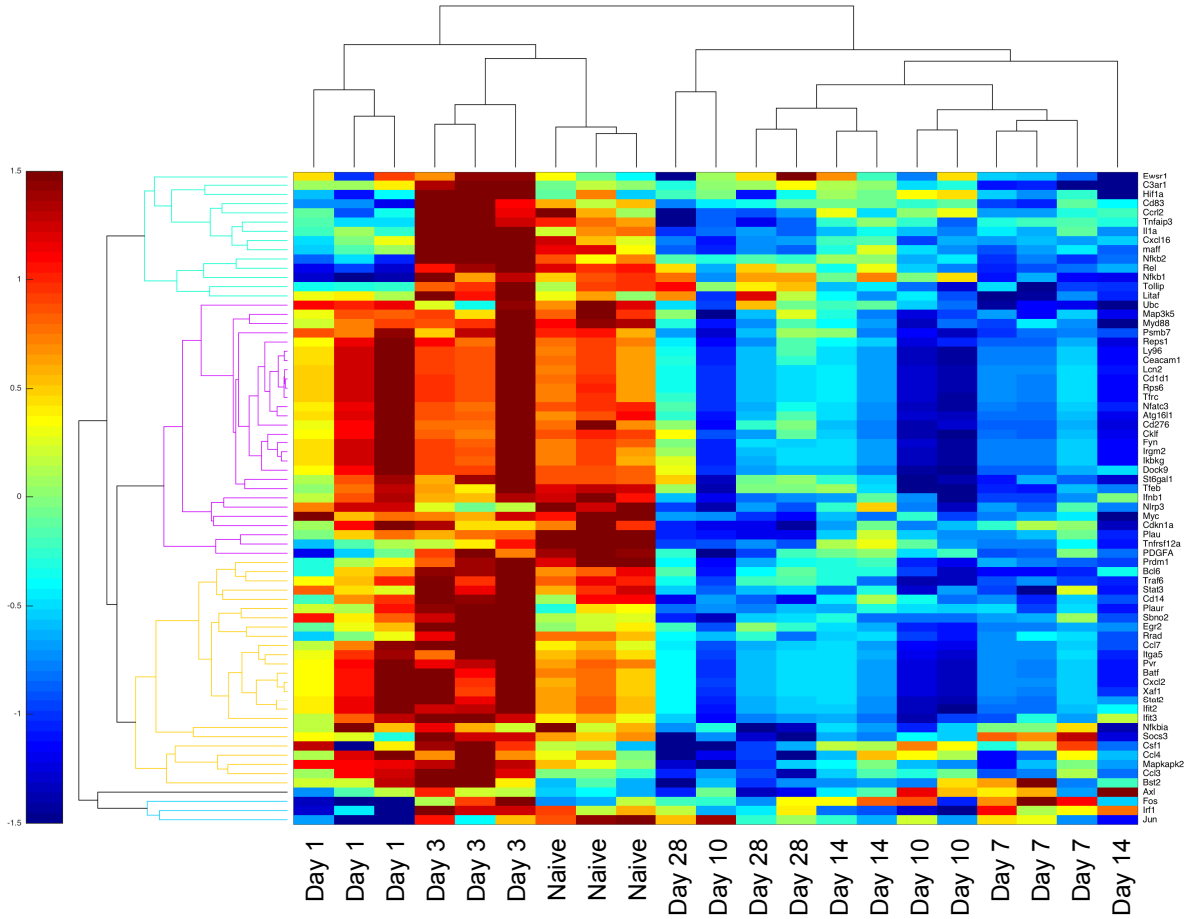

C) Clusters 5-7

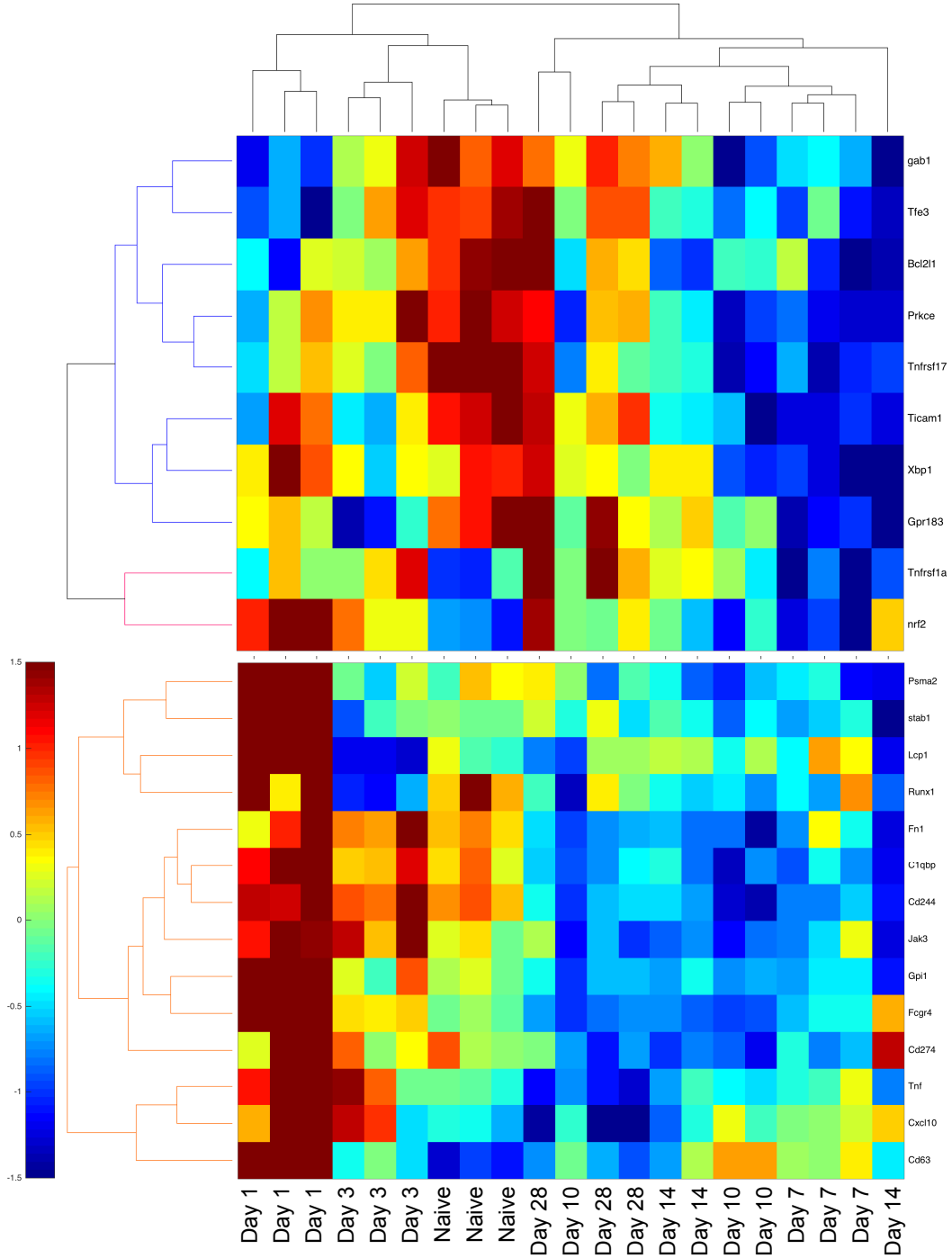

D) Clusters 8-11

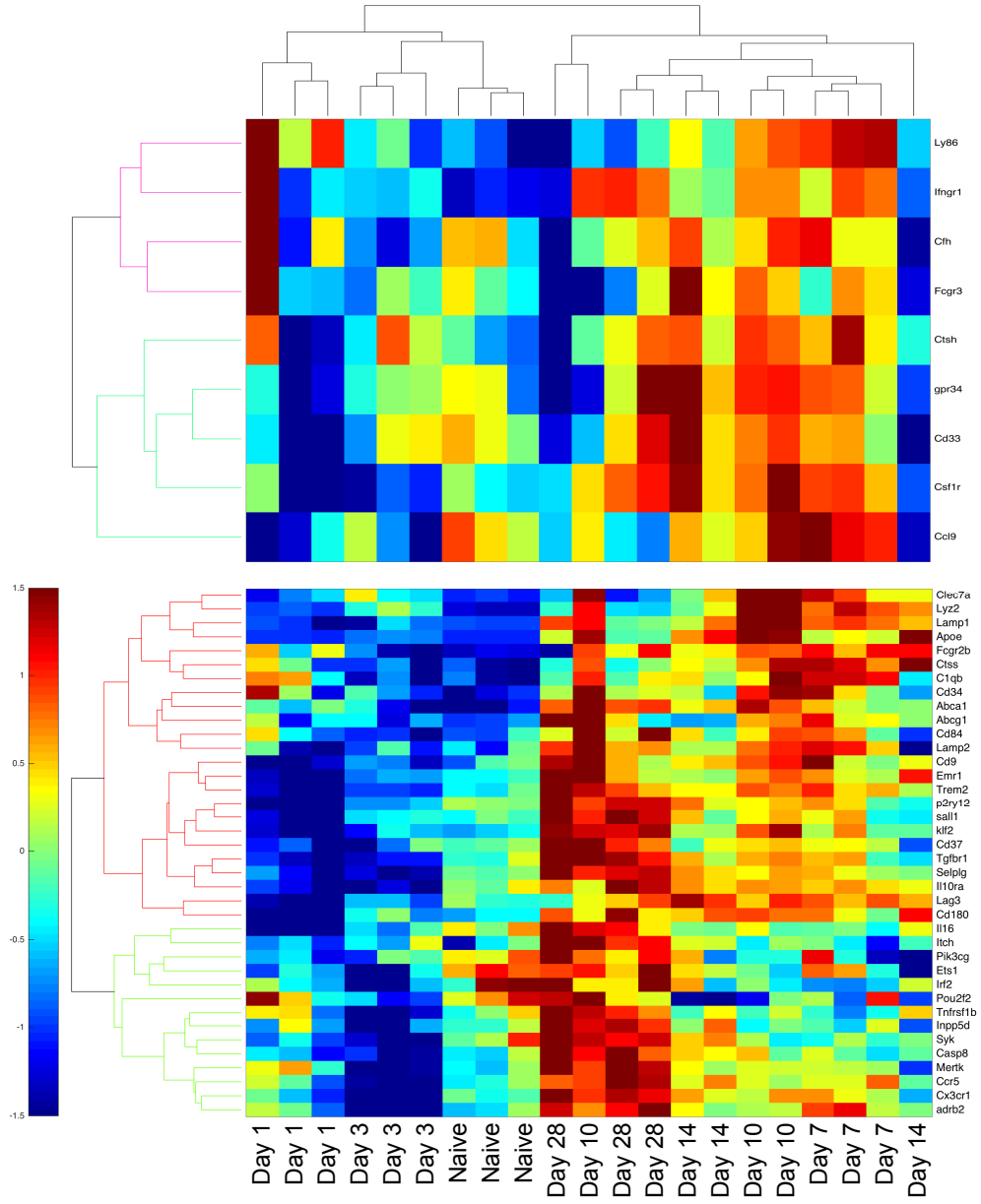

E) Clusters 12-13

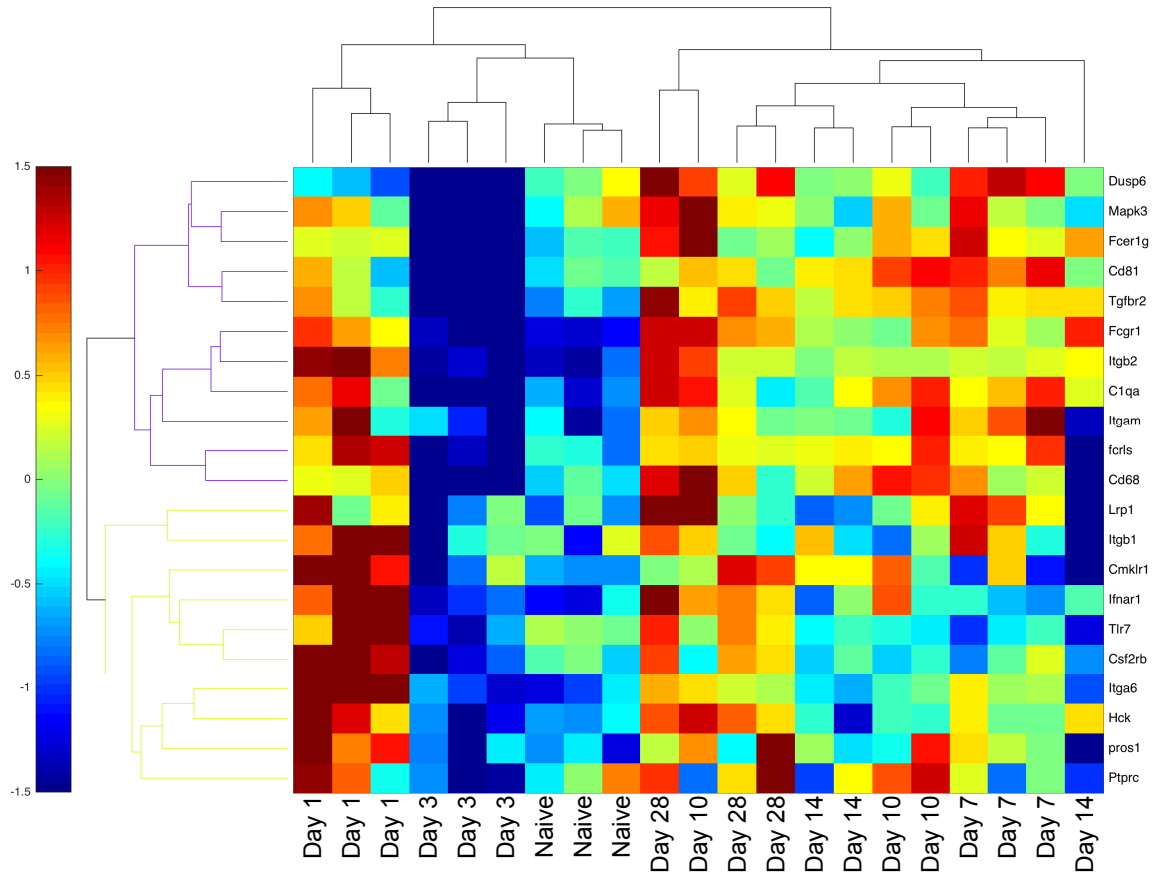

F) Clusters 14-15

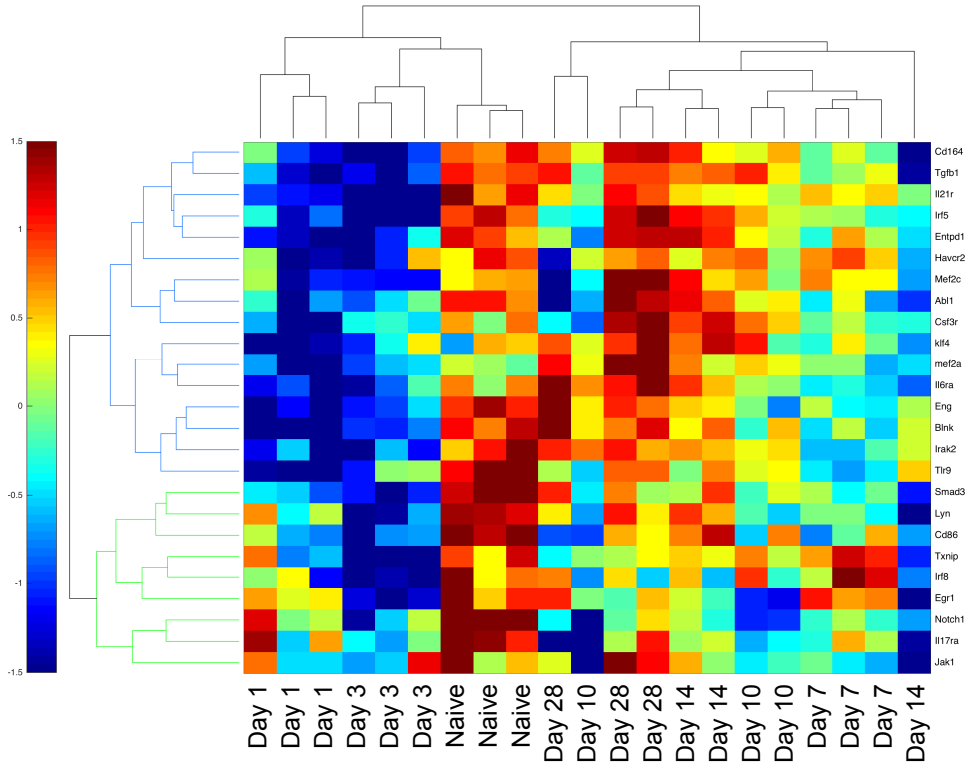

G)

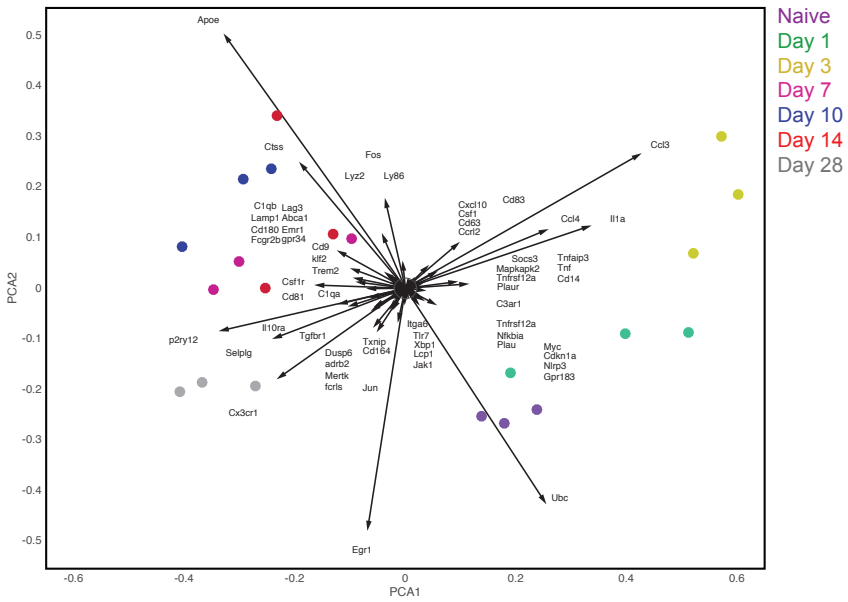

H)

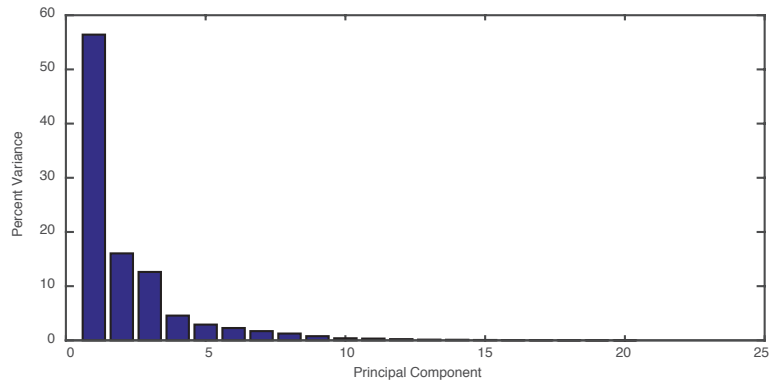

Supplemental Figure 1. Transcriptional analysis of microglia after ICH. Heat maps of all genes used for PCA. The entire filtered gene set is shown (A) followed by enlargements of each cluster for clarity (B-F). G) Scatter plot shows each sample projected on the first two principal components and are color coded according to time point. Genes are shown as projections along the first two components, and those that contribute significantly are labeled. Grey circle denotes the 90th percentile of coefficients. H) Percent variance explained by each principal component.

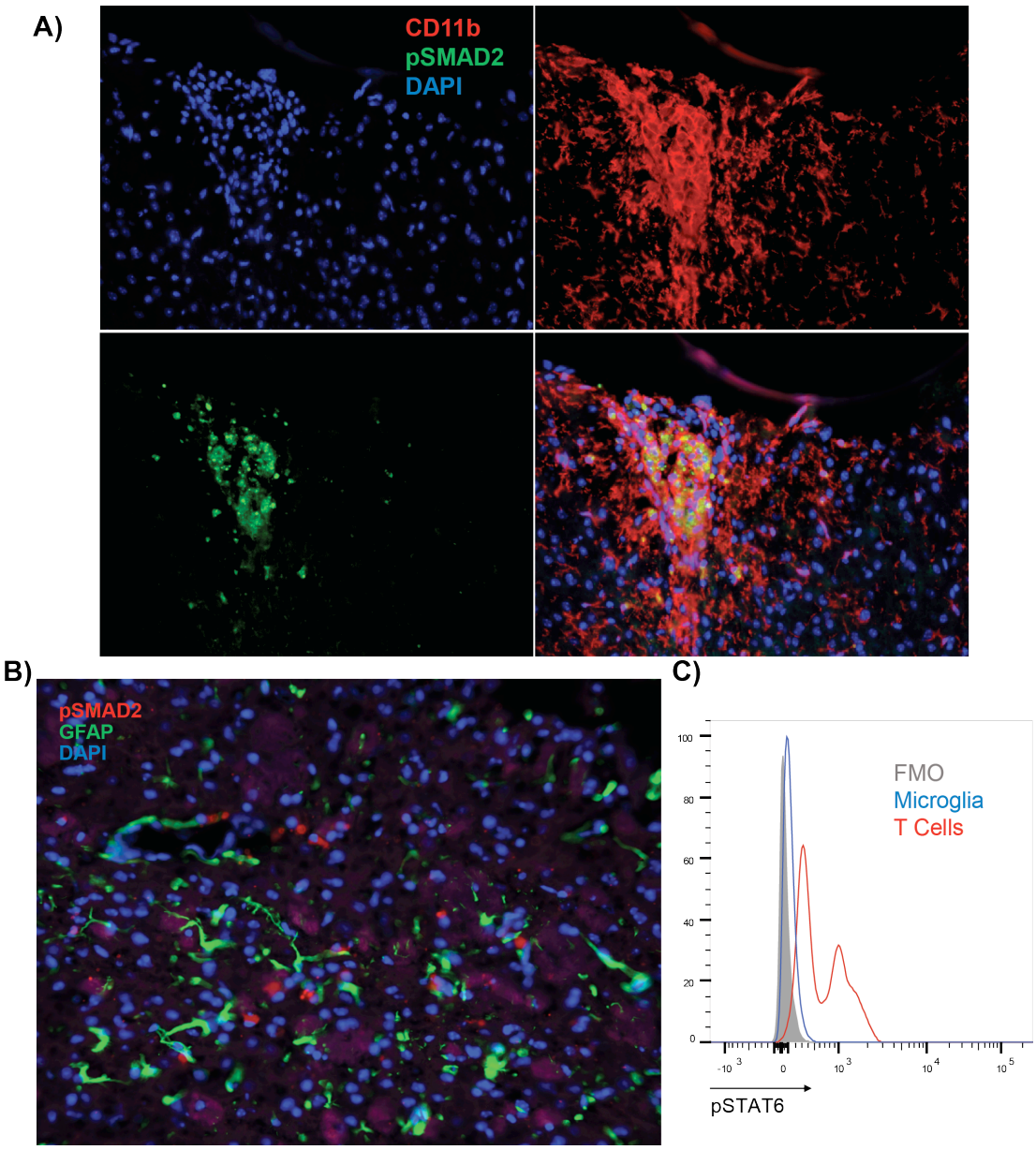

Supplemental Figure 2. CD11b+ cells signal through TGF-β1 14 days after ICH. A) Brain sections from WT mice were stained for CD11b (red), pSMAD2 (green), and nuclei were stained with Dapi. Representative image depicts a colocalization of CD11b and pSMAD2, suggesting myeloid cells signal through TGF-β1 at 14 days after ICH. **B)** Brain sections from WT mice were stained for GFAP (green), pSMAD2 (red), and nuclei were stained with Dapi. Representative image suggest that astrocytes do not signal via TGF-β1 14 days after ICH. 20x. n=4. **C)** Representative histogram suggests microglia (blue) do not signal through pSTAT6 at 7 days after ICH. T cells (red) are shown as a positive control, n=6.

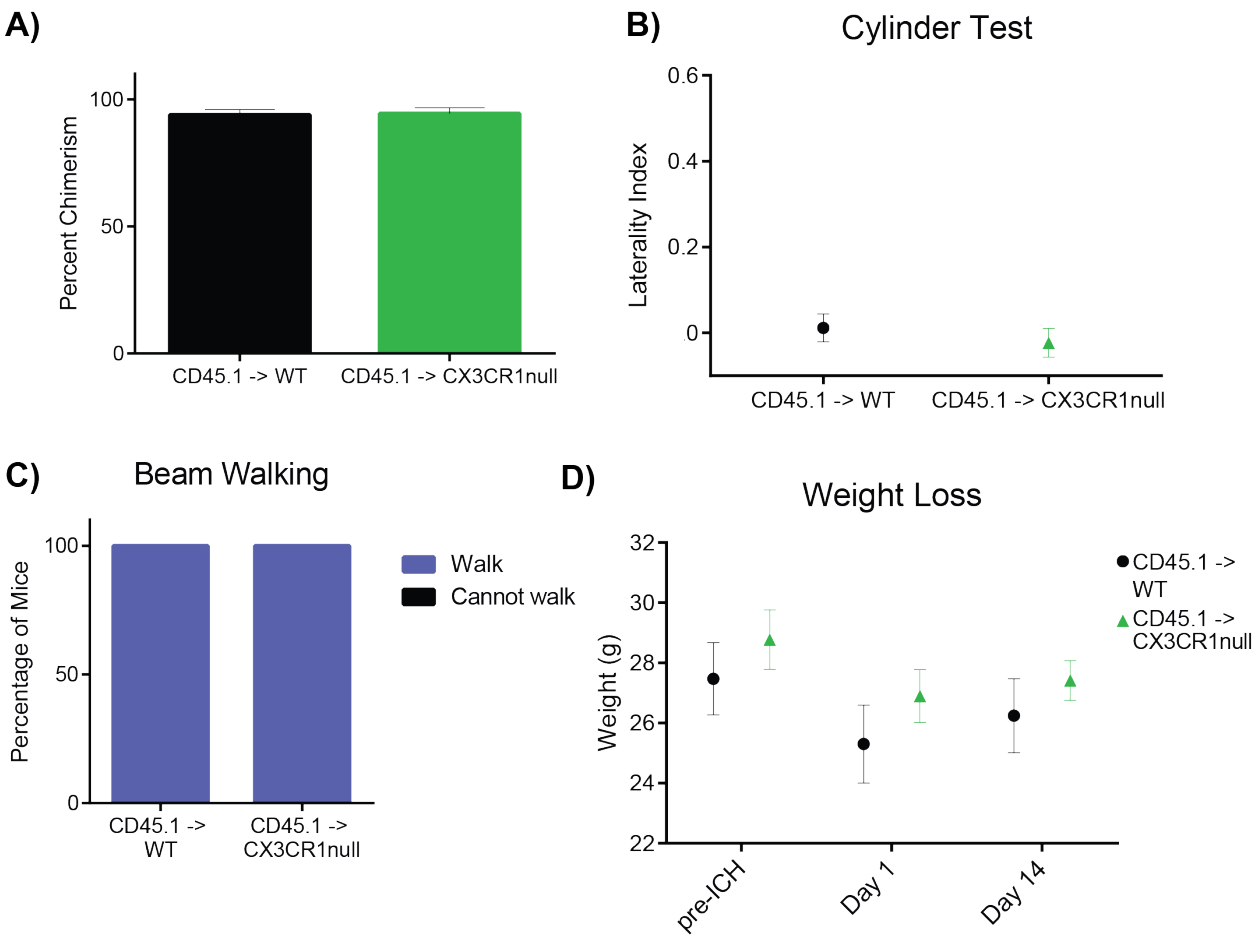

Supplemental Figure 3. There is no difference in naïve chimera behavior or weight loss after ICH. A) Percent chimerism of BM chimeras was measure by flow cytometry at 8 weeks after ICH. Graph depicts mean with s.e.m. n=12-13. **B-C)** Naïve WT and CX3CR1-null BM chimeras perform equally on cylinder test **(B)** and beam walking test **(C)**. Means graphed with s.e.m. n=8. **D)** There is no difference in weight loss between WT and CX3CR1-null BM chimeras 1 or 14 days after ICH. Means graphed with s.e.m. n=7-8.

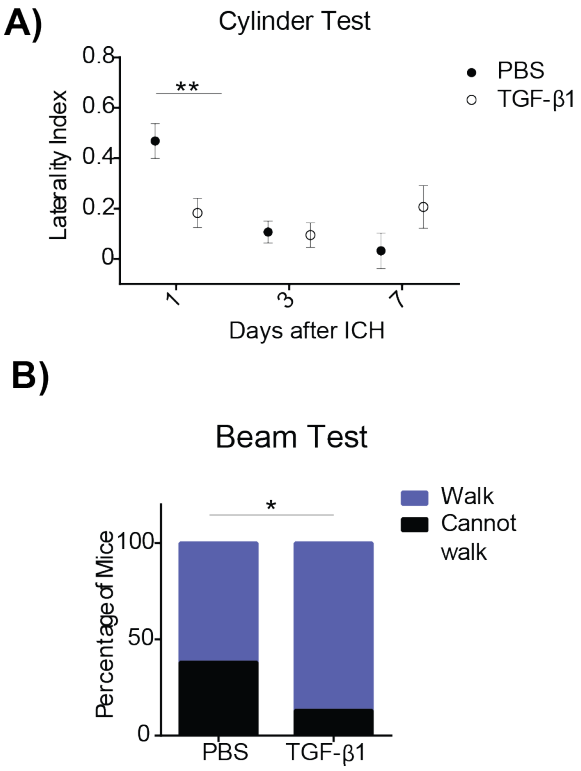

Supplemental Figure 4. Mice pretreated with TGF-β1 have better functional outcomes 24 hours after ICH. Mice were pre-treated with 10ng of TGF-β1 or PBS immediately prior to ICH surgery. **A)** Cylinder test results show that mice pre-treated with TGF-β1 had better functional outcomes on cylinder test at 24 hours compared to PBS treated mice. Means graphed with s.e.m. n=7-21. **B)** Mice were behavior tested on beam walking test 24 hours after ICH. Results showed that a greater percentage of TGF-β1 treated mice could walk on the beam compared to PBS treated. n=8. *$p<0.05$, **$p<0.01$.

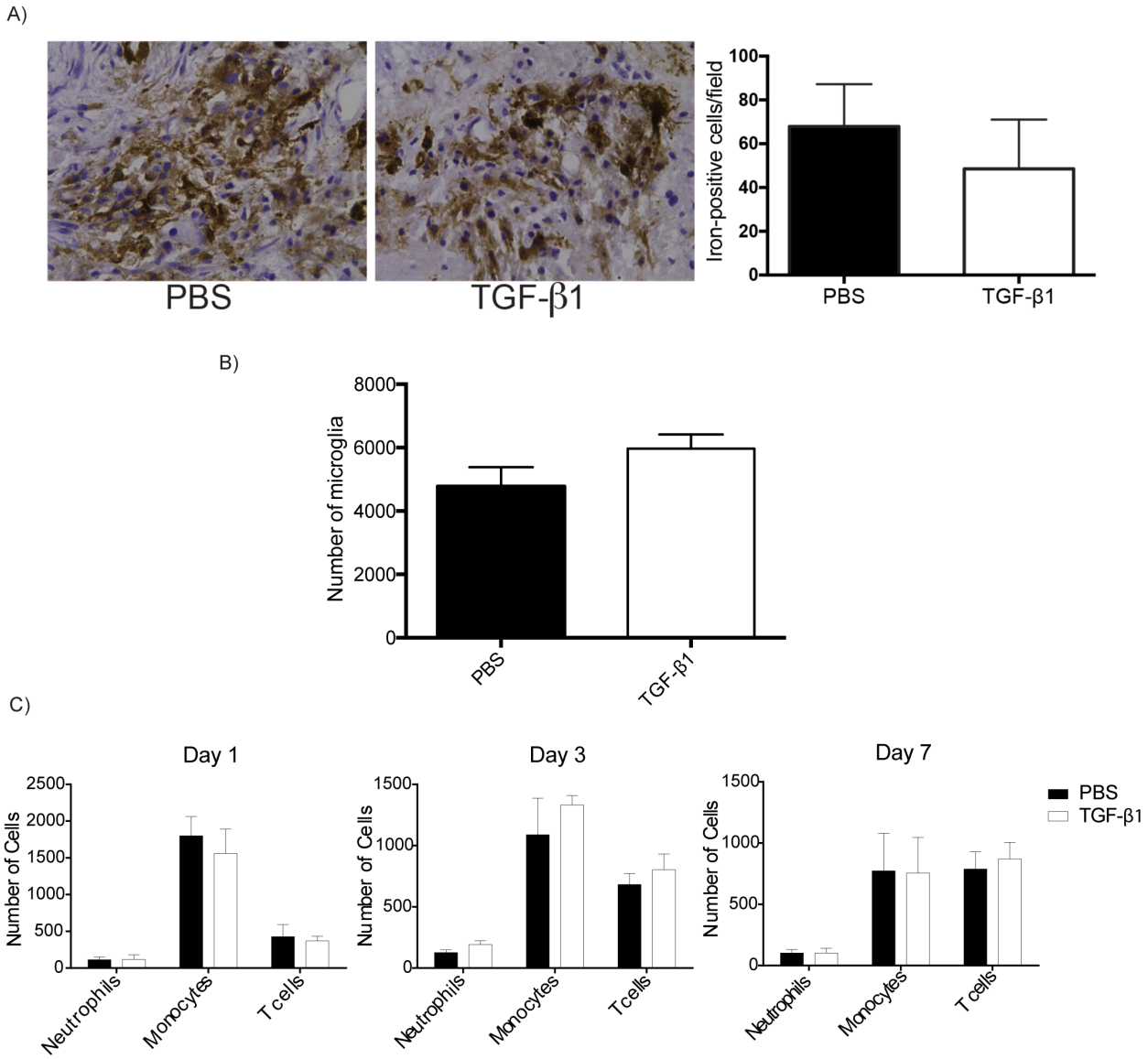

Supplemental Figure 5. There is no difference in iron phagocytosis, microglial numbers or leukocyte recruitment to the perihematomal region following TGF-β1 treatment at 4 hours after ICH. A) Brain sections from PBS and TGF-β1 mice were stained with Perls stain at 7 days after ICH. No differences were found in the number of iron positive cells, suggesting there is no majojr difference in hematoma phagocytosis between treatment groups. Means graphed with s.d. n=5. **B)** Perihematomal microglial numbers ($CD45^{int}$, $CD11b^{+}$ cells) were quantified by flow cytometry of mice 24 hours after ICH. No differences were observed in microglial numbers between PBS and TGF-β1 treatment. Means graphed with s.e.m. n=8. **C)** Monocyte, neutrophil and T cell recruitment to the perihematomal region was analyzed by flow cytometry 1, 3, and 7 days after ICH in mice that were treated with either TGF-β1 or PBS. Differences were not observed in monocyte, neutrophil, or T cell recruitment at any time point measured. Means graphed with s.e.m. n=4-6.

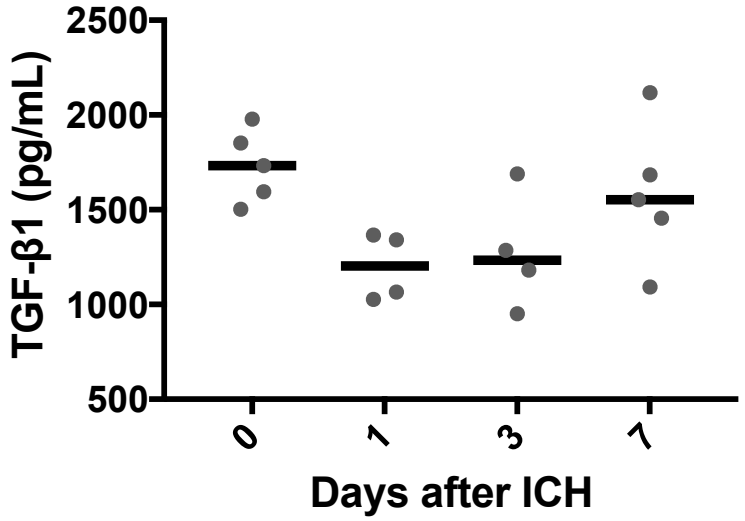

Supplemental Figure 6. TGF-β1 serum concentrations initially decrease and then return to baseline 7 days after ICH. TGF-β1 concentrations in mouse serum were measured in naïve animals, and 1, 3, and 7 days after ICH by ELISA assay. One day after ICH, TGF-β1 concentrations decreased and then returned to concentrations found in naïve mice 7 days after ICH. Individual mice graphed with line at the median. p=0.1 by ANOVA. n=4-5.

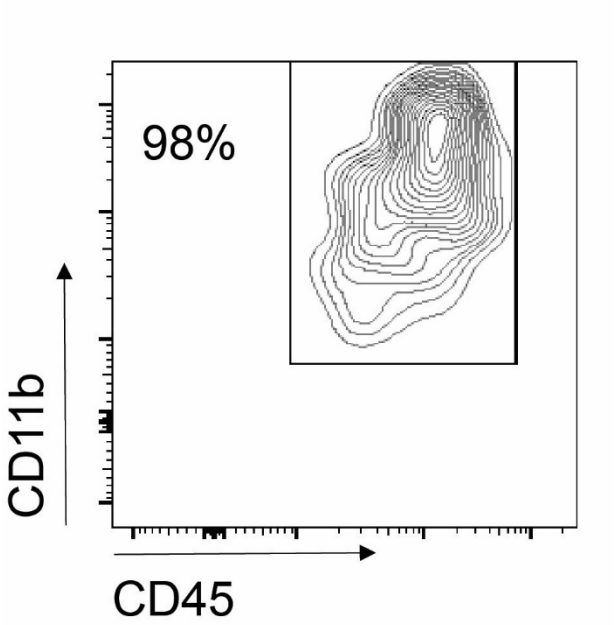

Supplemental Figure 7. Purity of primary microglial cultures. Microglia were shaken off of the astrocyte bed 14 days after mixed glial cultures were made. Microglia were harvested and an aliquot was run on a cytometer to measure cell purity. Representative flow plot shows that primary microglial cultures are 98% pure.

Supplemental Tables

Supplemental Table 1. Characteristics of intracerebral hemorrhage patients.

	ICH patients (n=22)	Controls (n=22)
Age	66.9 ± 10.3 years	66.0 ±14.2 years
History of hypertension	17 (73%)	14 (64%)
Intracerebral hemorrhage volume	22.1 ± 23.0 mL	
Initial NIH Stroke Scale Score	10 [4-19]	
Initial Glasgow Coma Scale score	14 [14-15]	
Intraventricular hemorrhage	10 (40%)	
Infratentorial location	2 (8%)	
External ventricular drain	4 (16%)	
Surgical evacuation	3 (12%)	
Infection in first 3 days	4 (16.7%)	
Hospitalization length	7.2 [5.2-19.3] days	
Modified Rankin Scale score at 90 days	3.3 ± 2.0	

Data presented as mean ± standard deviation when data is normally distributed, median [interquartile range] when data is not normally distributed, or as number (percentages). There were no differences in age and prevalence of hypertension between ICH patients and controls.

Supplemental Table 2: List of Primer Sequences

Gene	Forward	Reverse	Source
Actin	5'-CTAAGGCCAACCGTGAAAG-3'	5'-ACCAGAGGCATACAGGGACA-3'	[1]
BDNF	5'-CAAGAGTCCCGTCTGTACTTTAC-3'	5'-GACTAGGGAAATGGGCTTAACA-3'	
CCL2	5'-ATGCTTGGCTCAGCAC-3'	5'-TCAATTTTTCATTTTGAGTGT-3'	[2]
CD206	5'-CAAGGAAGGTTGGCATTTGT-3'	5'-CCTTTCAGTCCTTTGCAAGC-3'	[3]
IL-6	5'-AGGAGACTTCACAGAGGATACC-3'	5'-GAATTGCCATTGCACAACTCTT-3'	
SOCS3	5'-GTTGAGCGTCAAGACCCAGT-3'	5'-CACGTTGGAGGAGAGAGGTG-3'	[4]
TGFBR1	5'-TGCCATAACCGCACTGTCA-3'	5'-AATGAAAGGGCGATCTAGTGATG-3'	[5]
TNF	5'-CATCAGTTCTATGGCCCAGACCCT-3'	5'-GCTCCTCCACTTGGTGGTTTGCTA-3'	[6]

Supplemental References:

1. Simon DP, Giordano TJ, Hammer GD. Upregulated jag1 enhances cell proliferation in adrenocortical carcinoma. *Clinical cancer research : an official journal of the American Association for Cancer Research*. 2012;18:2452-2464
2. Izhak L, Wildbaum G, Weinberg U, Shaked Y, Alami J, Dumont D, et al. Predominant expression of ccl2 at the tumor site of prostate cancer patients directs a selective loss of immunological tolerance to ccl2 that could be amplified in a beneficial manner. *Journal of immunology (Baltimore, Md. : 1950)*. 2010;184:1092-1101
3. Wang G, Zhang J, Hu X, Zhang L, Mao L, Jiang X, et al. Microglia/macrophage polarization dynamics in white matter after traumatic brain injury. *J Cereb Blood Flow Metab*. 2013;33:1864-1874
4. Qin H, Wang L, Feng T, Elson CO, Niyongere SA, Lee SJ, et al. Tgf-beta promotes th17 cell development through inhibition of socs3. *Journal of immunology (Baltimore, Md. : 1950)*. 2009;183:97-105
5. Li S, Miller CH, Giannopoulou E, Hu X, Ivashkiv LB, Zhao B. Rbp-j imposes a requirement for itam-mediated costimulation of osteoclastogenesis. *J Clin Invest*. 2014;124:5057-5073
6. Nakazawa T, Nakazawa C, Matsubara A, Noda K, Hisatomi T, She H, et al. Tumor necrosis factor-alpha mediates oligodendrocyte death and delayed retinal ganglion cell loss in a mouse model of glaucoma. *J Neurosci*. 2006;26:12633-12641